

Figure 2 Schematic representation of the simulated HYBRID model interfaces and potential density (referenced to 2000 dbar). (a) Meridional section along 148°E showing vertical grid interfaces overlaid on potential density (kg m⁻³). (b) Zonal section along 36°N across the Yellow Sea, illustrating the vertical grid structure adapted to shallow topography.

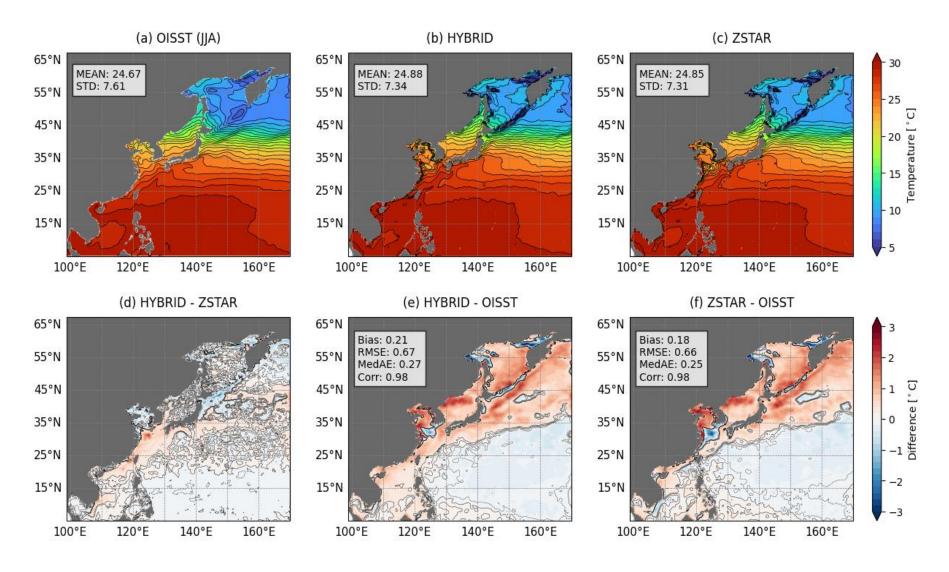


Figure 3. Boreal winter (DJF) mean sea surface temperature (SST) distributions from OISST observations and HYBRID and ZSTAR simulations. (a–c) Spatial SST distributions with corresponding means STD. (d) Differences between HYBRID and ZSTAR. (e, f) Biases relative to OISST, including Bias, RMSE, MedAE, and Corr. Contour lines in (d–f) indicate SST biases ranging from -0.1 to 0.1 °C at 0.1 °C intervals.

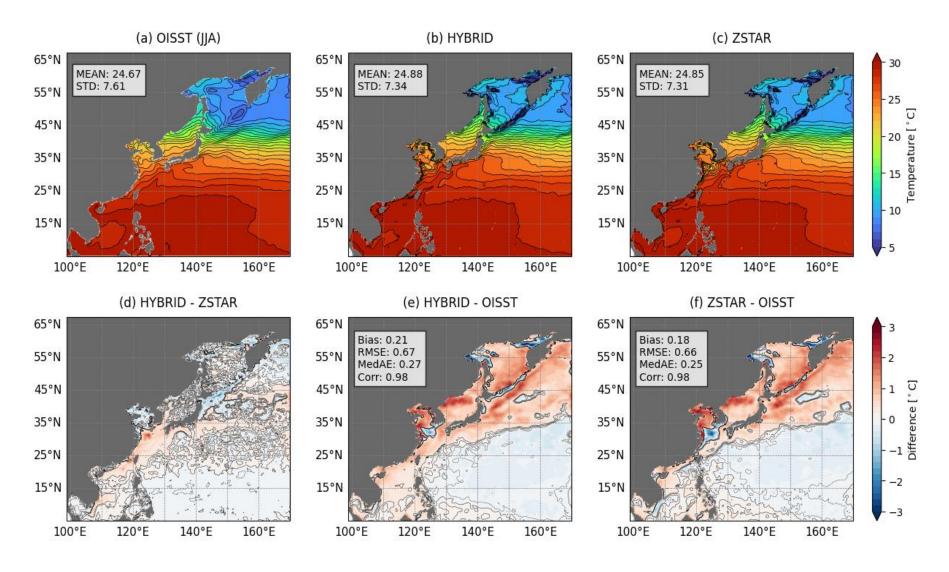


Figure 4. Boreal summer (JJA) mean sea surface temperature (SST) distributions from OISST observations and HYBRID and ZSTAR simulations. (a–c) Spatial SST distributions with corresponding means and STD. (d) Differences between HYBRID and ZSTAR. (e, f) Biases relative to OISST, including Bias, RMSE, MedAE, and Corr. Contour lines in (d–f) indicate SST biases ranging from -0.1 to 0.1 °C at 0.1 °C intervals.

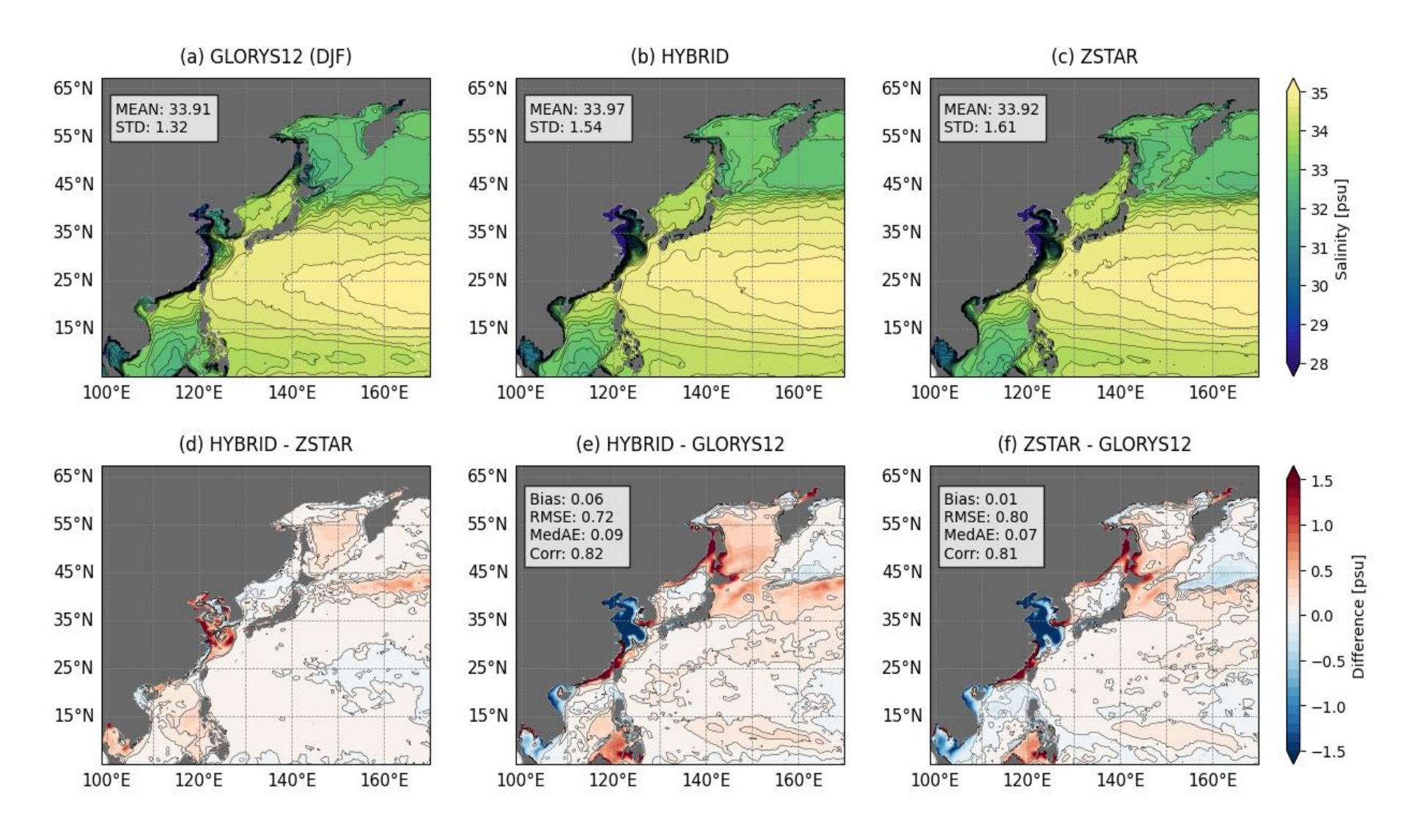


Figure 5. Boreal winter (DJF) mean sea surface salinity (SSS) distributions from the GLORYS12 reanalysis and HYBRID and ZSTAR simulations. (a–c) Spatial SSS distributions with corresponding means and STD. (d) Differences between HYBRID and ZSTAR. (e, f) Biases relative to GLORYS12, including Bias, RMSE, MedAE, and Corr. Contour lines in (d–f) indicate SSS biases ranging from -0.1 to 0.1 psu at 0.1 psu intervals.

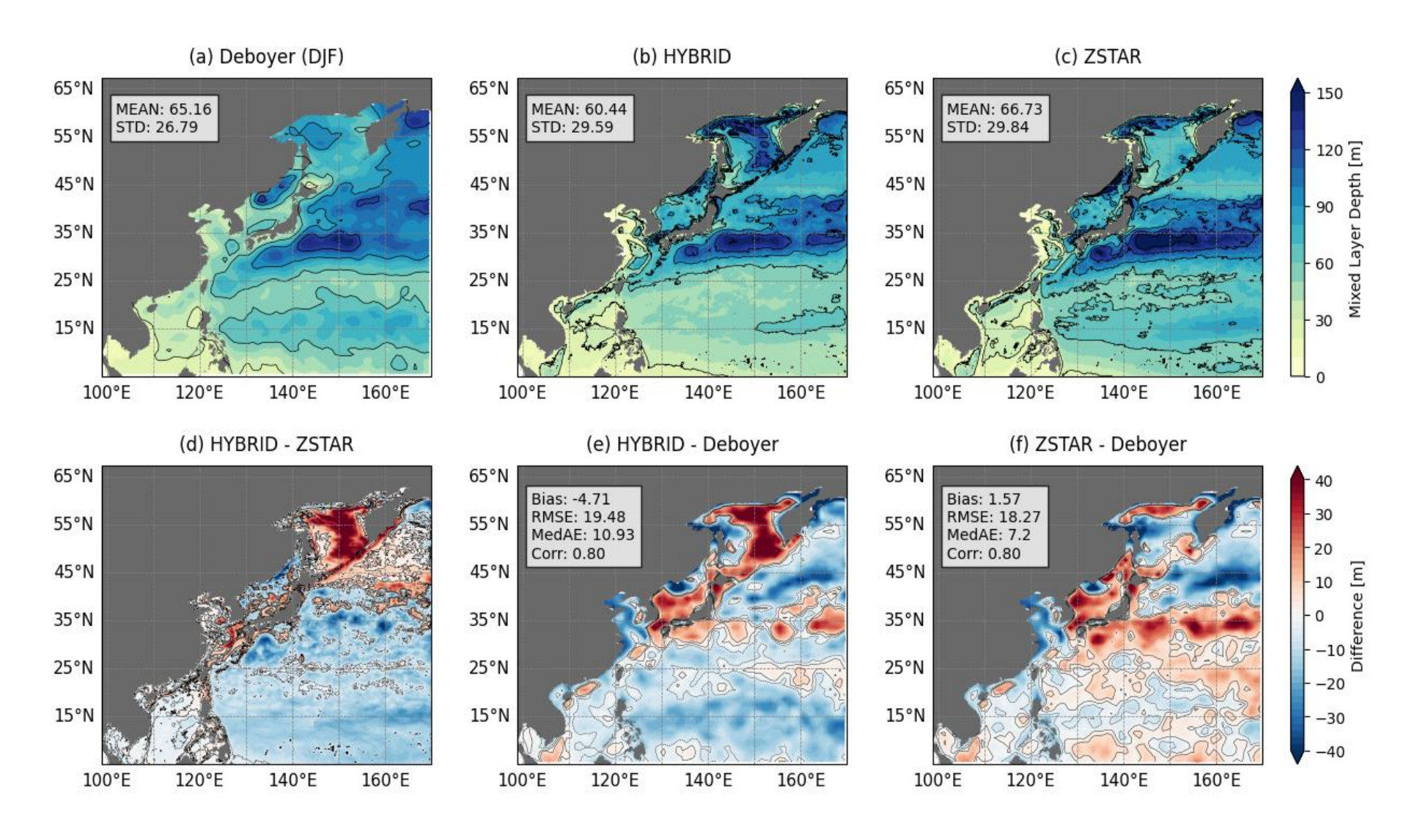


Figure 6. Boreal winter (DJF) mean mixed layer depth (MLD) distributions from de Boyer Montégut and HYBRID and ZSTAR simulations. (a–c) Spatial MLD distributions with corresponding means and STD. (d) Differences between HYBRID and ZSTAR. (e, f) Biases relative to de Boyer Montégut, including Bias, RMSE, MedAE, and Corr. Contour lines in (d–f) indicate MLD biases ranging from -0.1 to 0.1 m at 0.1 m intervals.

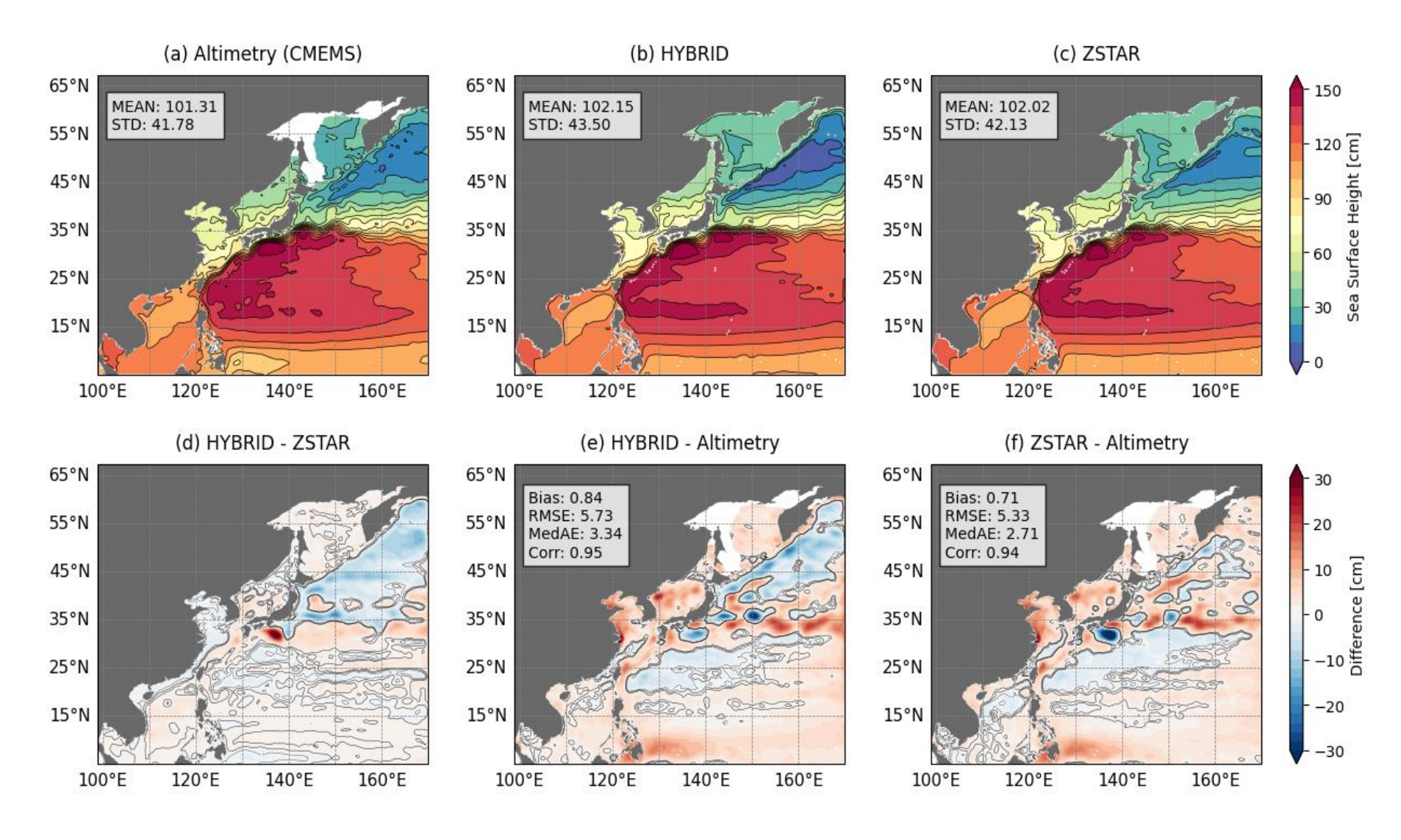


Figure 7. Mean sea surface height (SSH) distributions from Altimetry data and HYBRID and ZSTAR simulations. (a–c) Spatial SSH distributions with corresponding means and STD. (d) Differences between HYBRID and ZSTAR. (e, f) Biases relative to Altimetry, including Bias, RMSE, MedAE, and Corr. Contour lines in (d–f) indicate SSH biases ranging from -1.0 to 1.0 cm at 1.0 cm intervals.

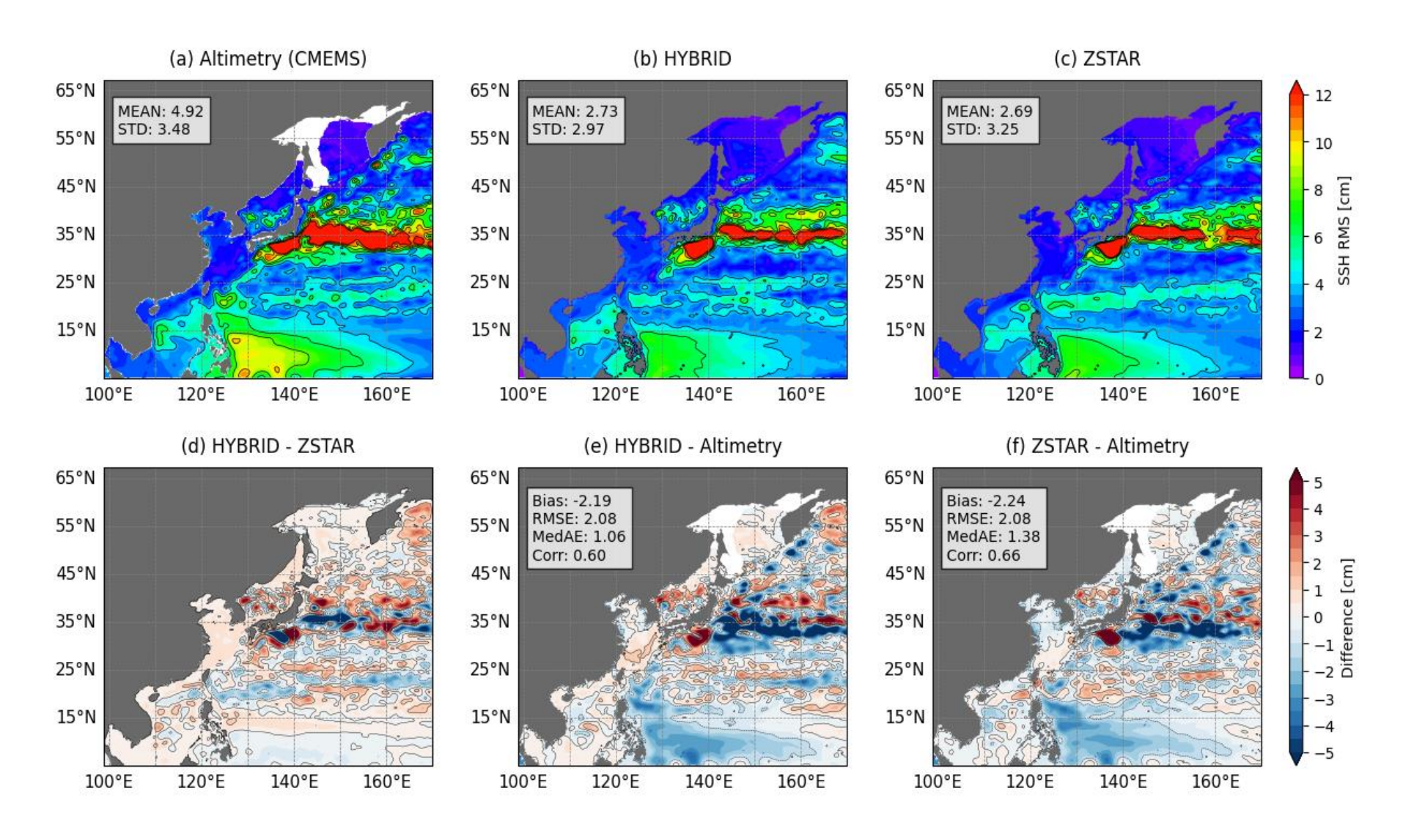


Figure 9. Root-mean-square (RMS) sea surface height (SSH) variability from high-pass filtered Altimetry data and HYBRID and ZSTAR simulations. (a–c) Spatial RMS SSH distributions with corresponding means and STD. (d) Differences between HYBRID and ZSTAR. (e, f) Biases relative to Altimetry, including Bias, RMSE, MedAE, and Corr. Contour lines in (d–f) indicate RMS SSH biases ranging from -1.0 to 1.0 cm at 1.0 cm intervals.

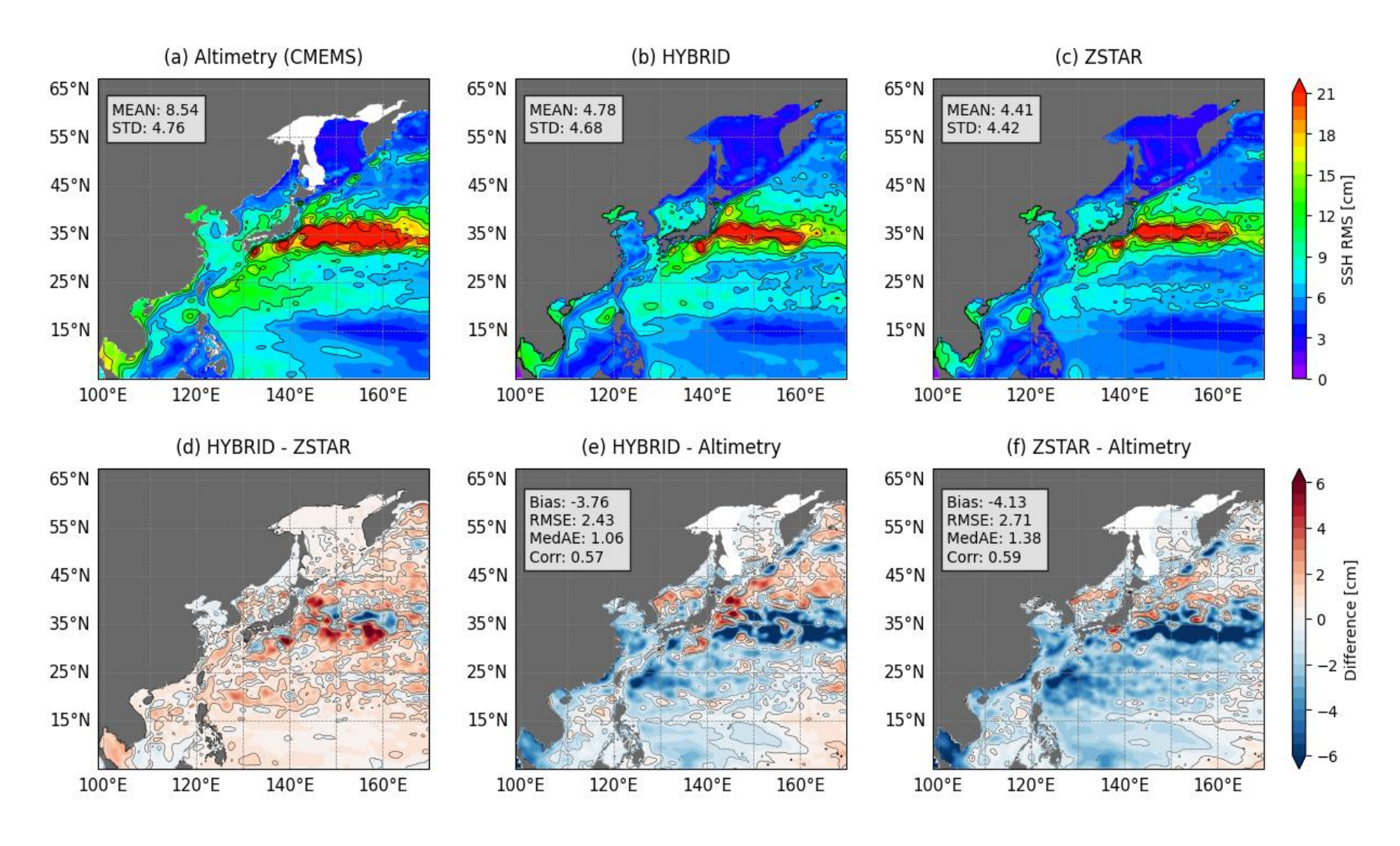


Figure 8. Root-mean-square (RMS) sea surface height (SSH) variability from low-pass filtered Altimetry data and HYBRID and ZSTAR simulations. (a–c) Spatial RMS SSH distributions with corresponding means and STD. (d) Differences between HYBRID and ZSTAR. (e, f) Biases relative to Altimetry, including Bias, RMSE, MedAE, and Corr. Contour lines in (d–f) indicate RMS SSH biases ranging from -1.0 to 1.0 cm at 1.0 cm intervals.

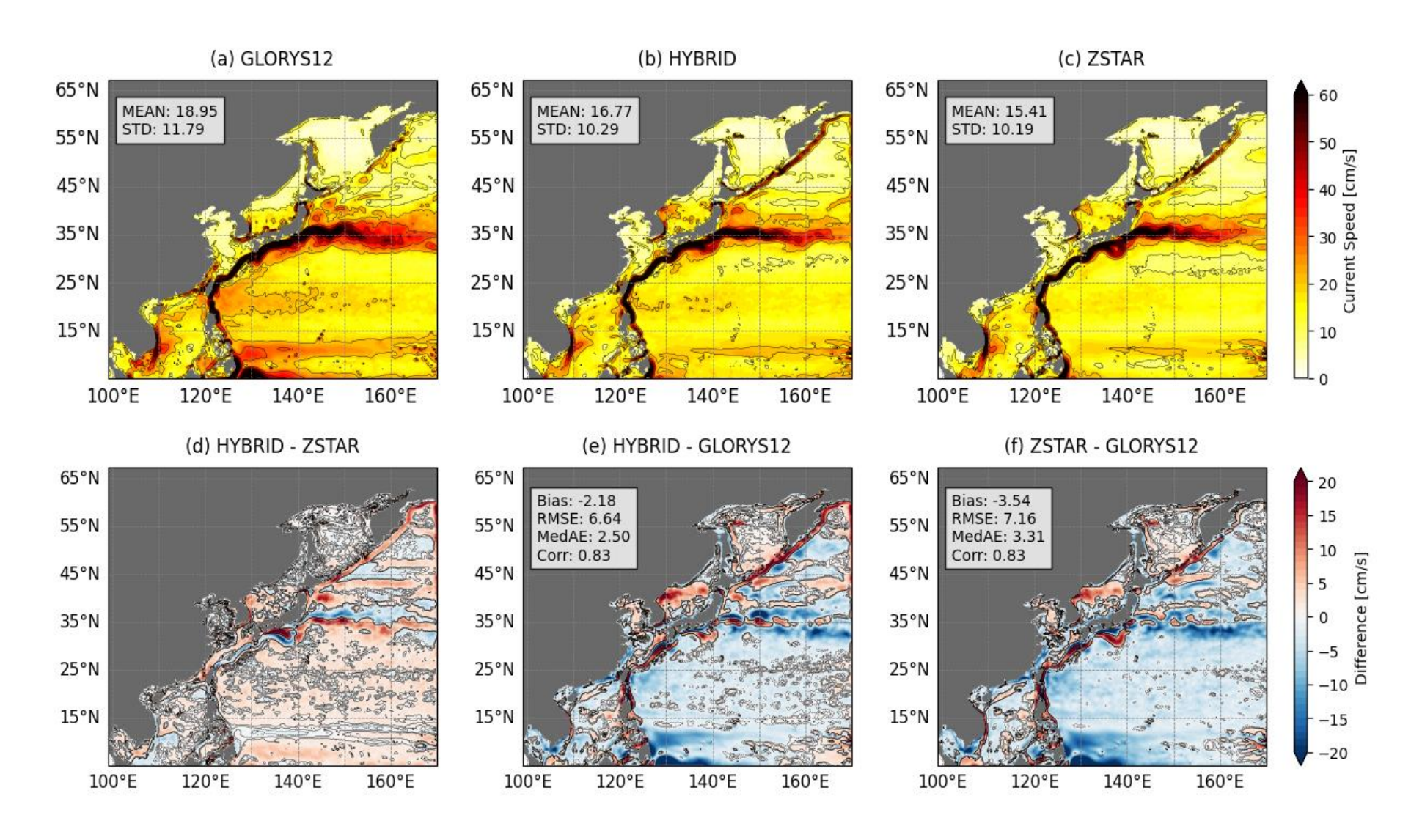


Figure 10. Mean surface current speed from GLORYS12, HYBRID, and ZSTAR simulations. (a–c) Spatial distributions of surface current speed with corresponding means and STD. (d) Differences between HYBRID and ZSTAR. (e, f) Biases relative to GLORYS12, including Bias, RMSE, MedAE, and Corr. Contour lines in (d–f) indicate surface current speed biases ranging from -1.0 to 1.0 cm/s at 1.0 cm/s intervals.

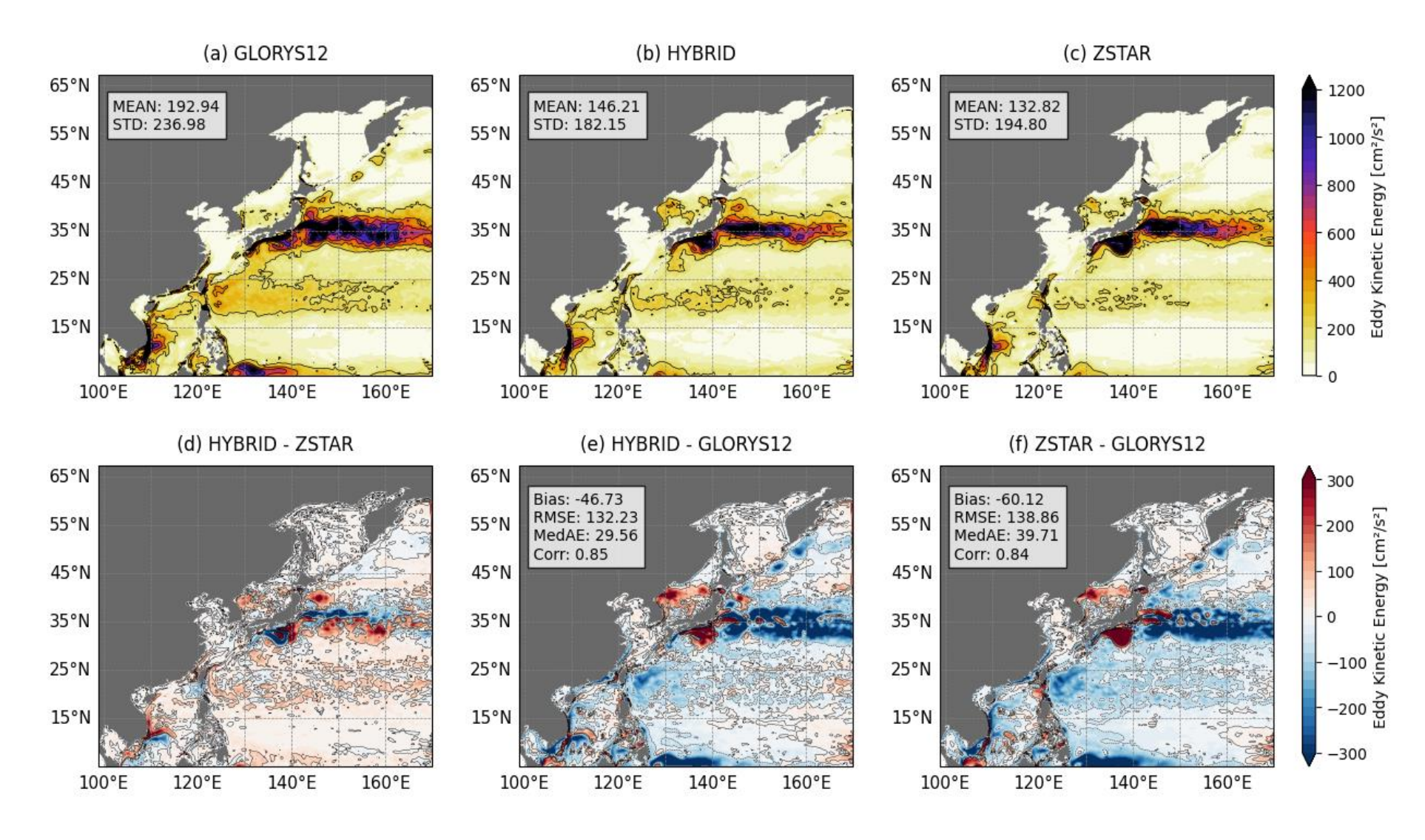
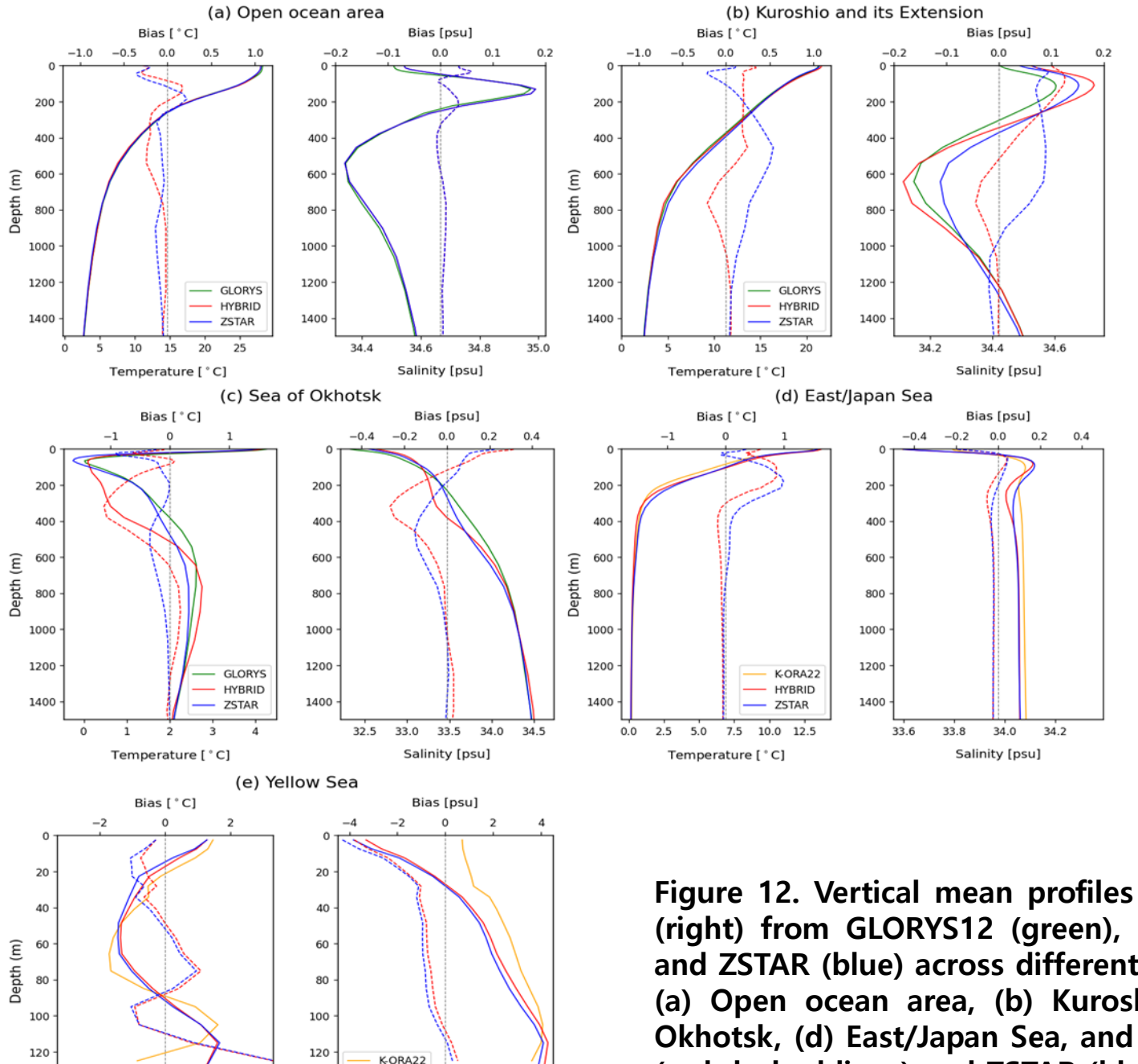


Figure 11. Mean eddy kinetic energy (EKE) from GLORYS12, HYBRID, and ZSTAR simulations. (a–c) Spatial EKE distributions with corresponding means and STD. (d) Differences between HYBRID and ZSTAR. (e, f) Biases relative to GLORYS12, including Bias, RMSE, MedAE, and Corr. Contour lines in (d–f) indicate EKE biases ranging from -0.5 to 1.0 cm²/s² at 0.5 cm²/s² intervals.



HYBRID

Salinity [psu]

ZSTAR

140

0 12 14 1
Temperature [° C]

Figure 12. Vertical mean profiles of temperature (left) and salinity (right) from GLORYS12 (green), K-ORA22 (orange), HYBRID (red), and ZSTAR (blue) across different Northwest Pacific (NWP) regions: (a) Open ocean area, (b) Kuroshio and its Extension, (c) Sea of Okhotsk, (d) East/Japan Sea, and (e) Yellow Sea. Biases for HYBRID (red dashed lines) and ZSTAR (blue dashed lines) are shown relative to the reference datasets (GLORYS12 or K-ORA22).

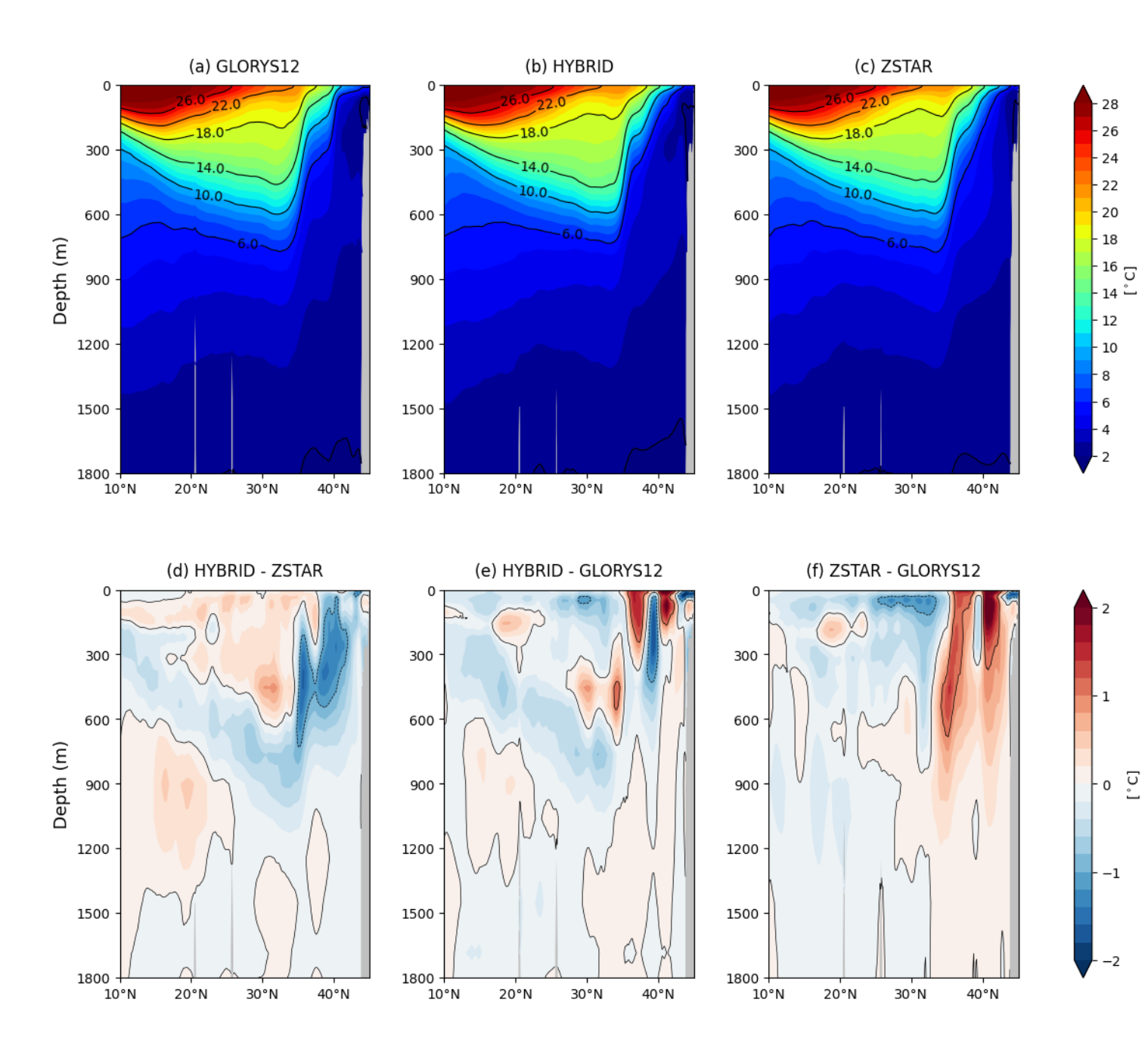


Figure 13 Meridional temperature section along 148°E from (a) GLORYS12 reanalysis, (b) HYBRID simulation, and (c) ZSTAR simulation, showing vertical temperature distribution. Panels (d), (e), and (f) illustrate temperature differences: HYBRID vs. ZSTAR (d), HYBRID vs. GLORYS12 (e), and ZSTAR vs. GLORYS12 (f). Contour lines in (d–f) indicate temperature biases ranging from -1.0 to 1.0 °C at 1.0 °C intervals.

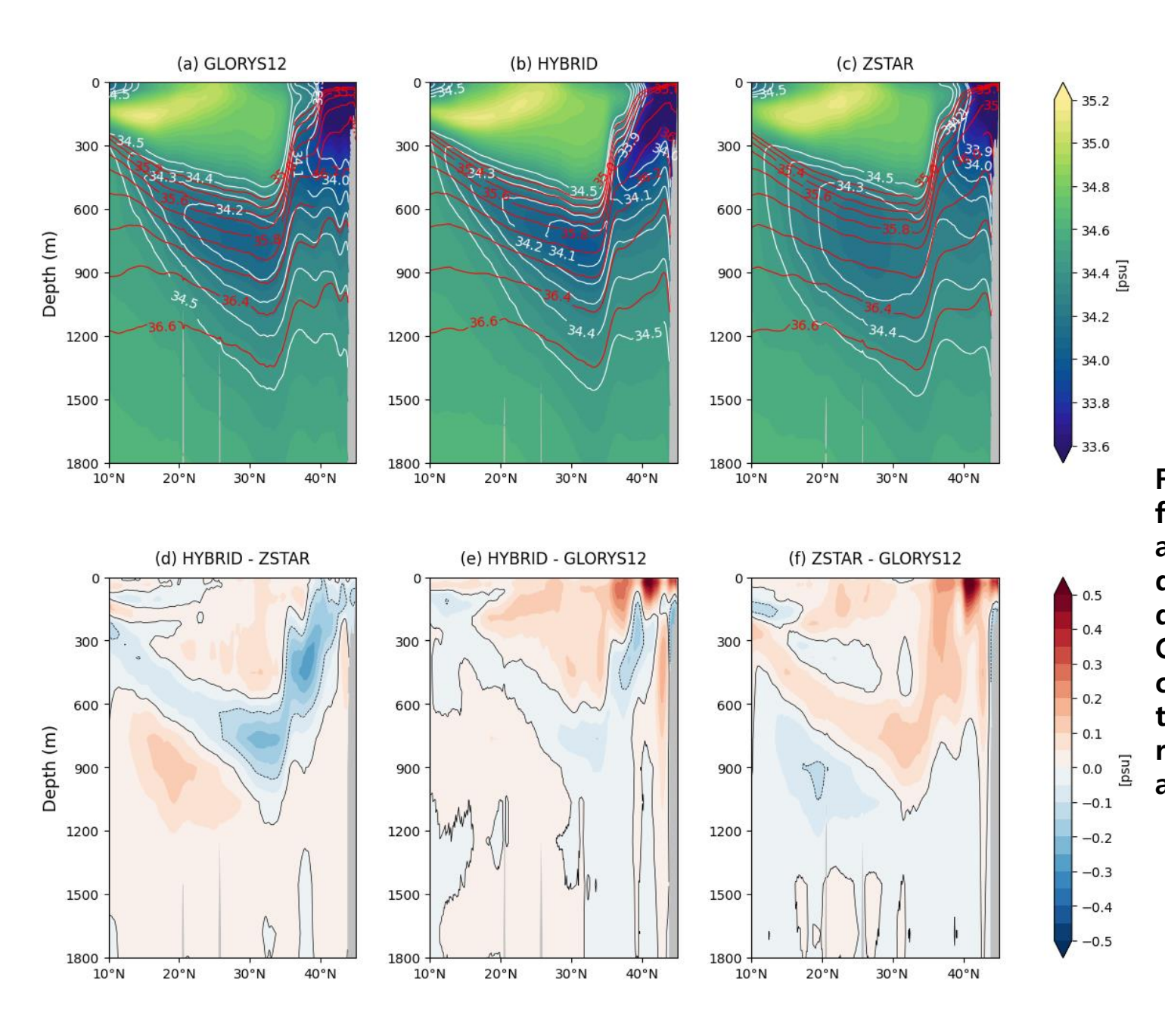


Figure 14 Meridional salinity section along $148^{\circ}E$ from (a) GLORYS12 reanalysis, (b) HYBRID simulation, and (c) ZSTAR simulation, showing vertical salinity distribution. Panels (d), (e), and (f) display salinity differences: HYBRID vs. ZSTAR (d), HYBRID vs. GLORYS12 (e), and ZSTAR vs. GLORYS12 (f). Red contour lines in (a–c) indicate σ_2 (density referenced to 2000 dbar) for each dataset. Contour lines in (d–f) represent salinity biases ranging from -0.1 to 0.1 psu at 0.1 psu intervals.

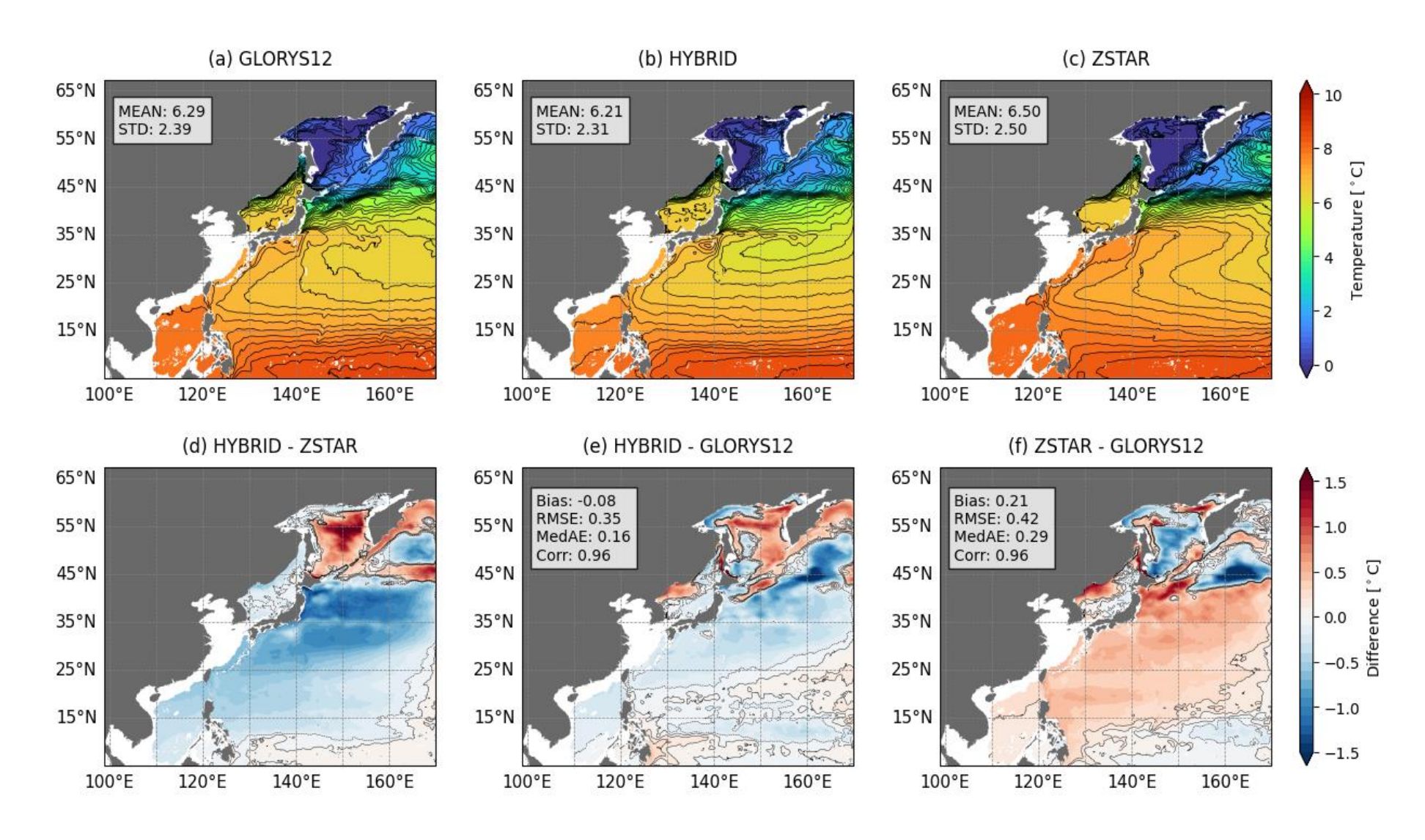


Figure 15 Temperature distributions at depths corresponding to σ_2 = 35.8 from (a) GLORYS12, (b) HYBRID, and (c) ZSTAR simulations, along with their respective means and STD. (d) Differences between HYBRID and ZSTAR. (e, f) Biases relative to GLORYS12, including Bias, RMSE, MedAE, and Corr. Contour lines in (d–f) indicate temperature biases ranging from -0.1 to 0.1 °C at 0.1 °C intervals.

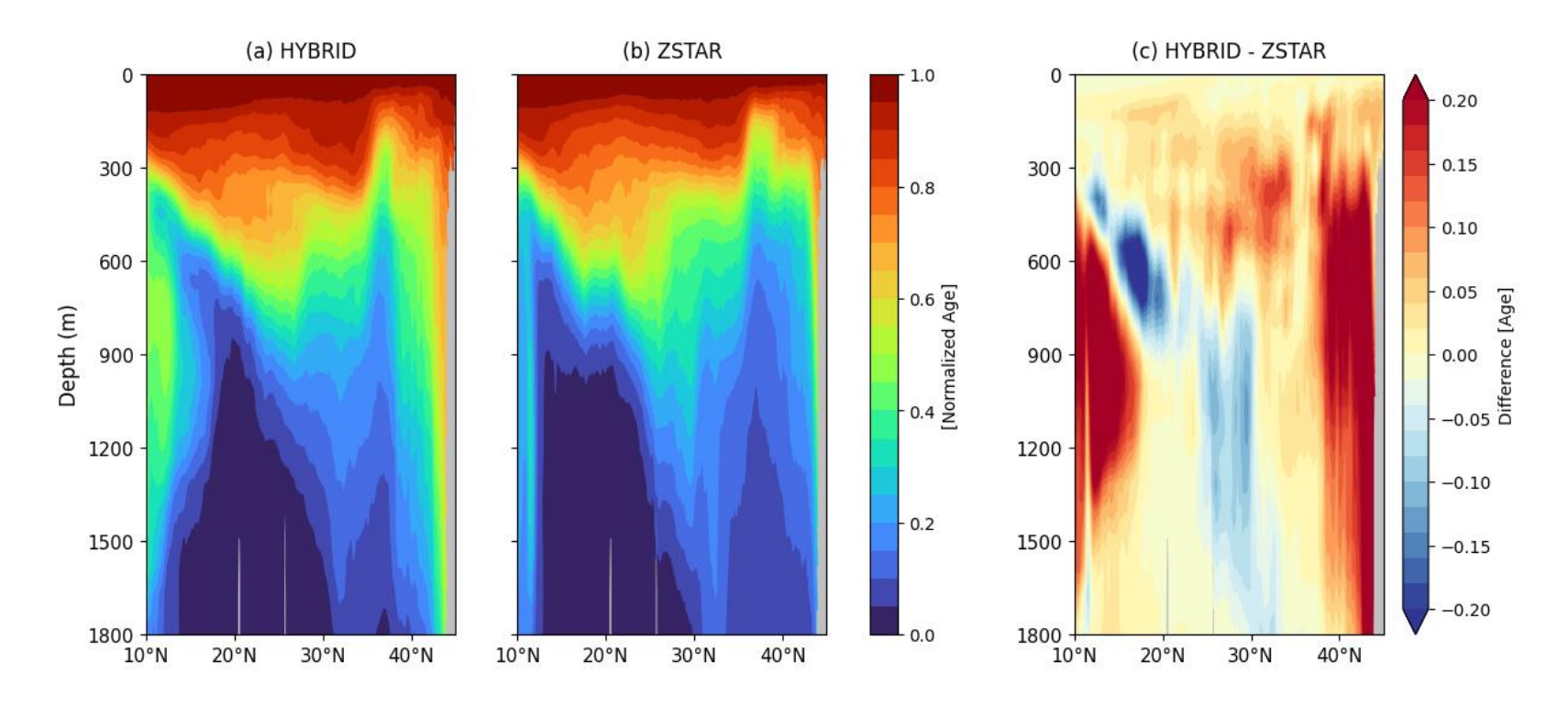


Figure 16. Meridional normalized age tracer along 148°E for (a) HYBRID, (b) ZSTAR, and (c) their difference (HYBRID - ZSTAR). The normalized age is computed as f=(A_max-A)/A_max, where A_max is the maximum age in the simulation, following Adcroft et al. (2019). Values range from 0 (oldest water) to 1 (youngest water), representing the relative ventilation age of water masses.

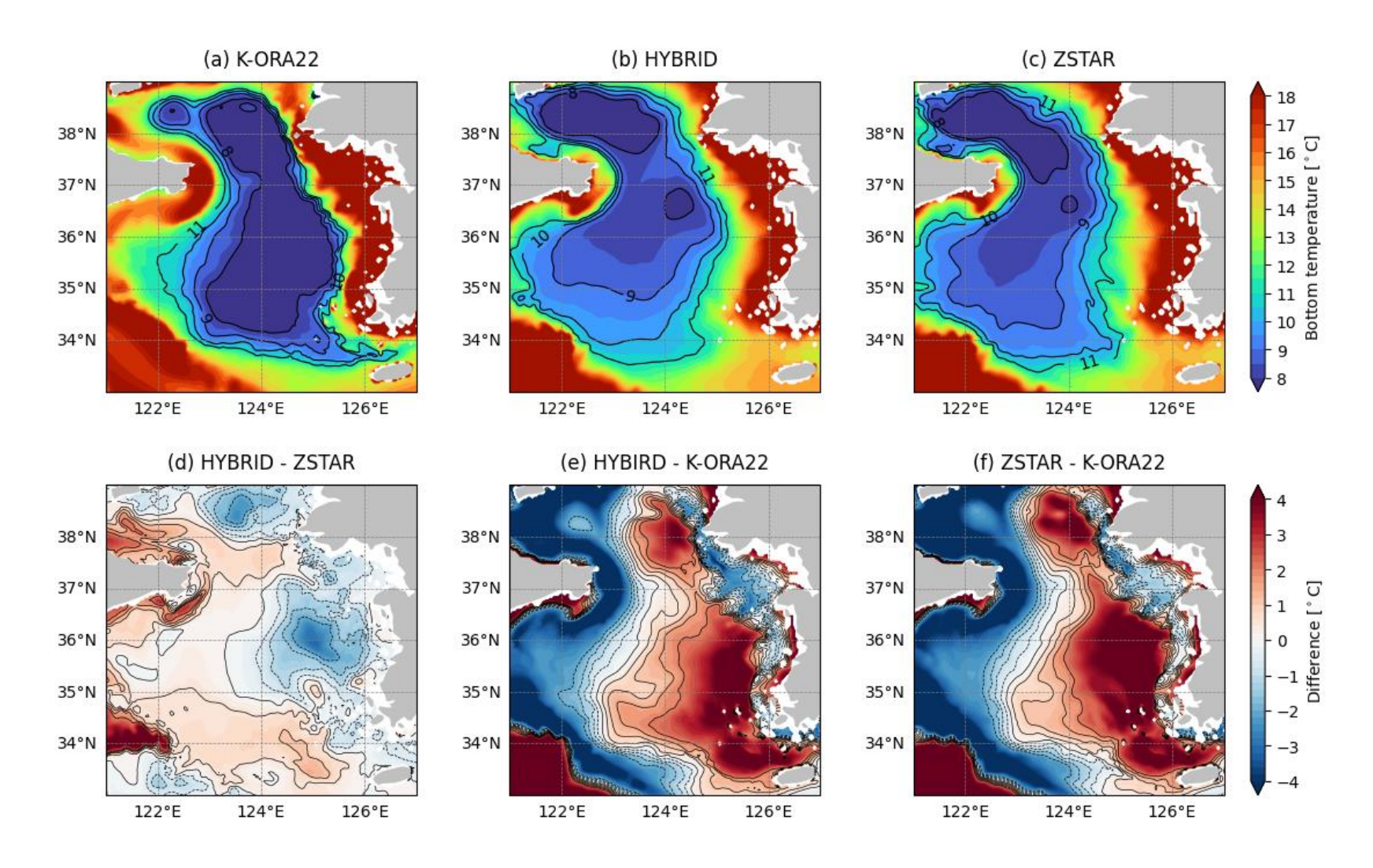


Figure 17. Bottom temperature distributions in the Yellow Sea from (a) K-ORA22, (b) HYBRID, and (c) ZSTAR simulations. (d) Temperature difference between HYBRID and ZSTAR. (e, f) Biases relative to K-ORA22. Contour lines in (d–f) indicate temperature biases ranging from -2.0 to 2.0 °C at 0.5 °C intervals.

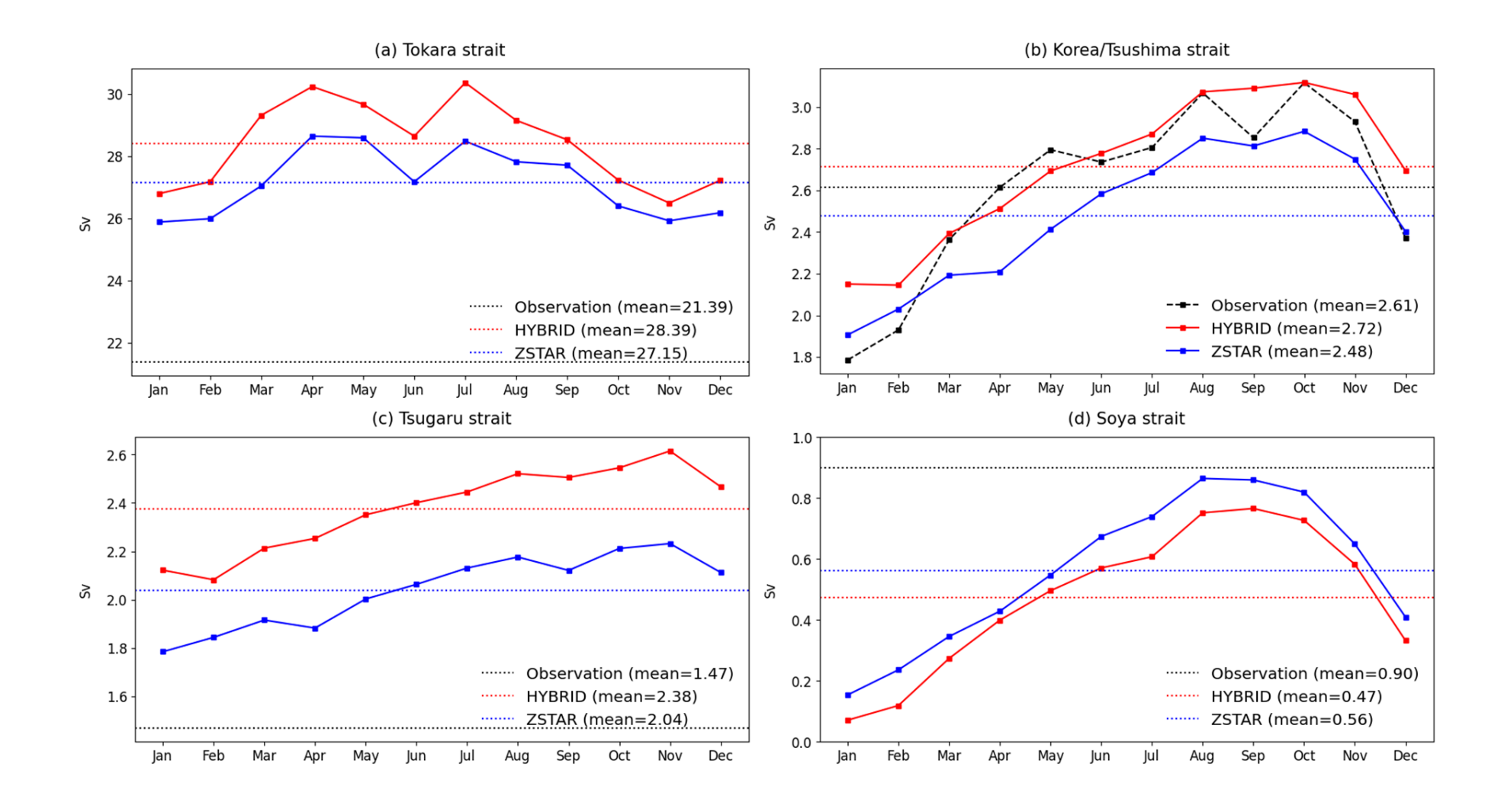


Figure 18. Monthly climatological mean volume transport at (a) Tokara Strait, (b) Korea/Tsushima Strait, (c) Tsugaru Strait, and (d) Soya Strait. Observations (black) are compared with HYBRID (red) and ZSTAR (blue). Dotted lines represent the annual mean for each dataset, while solid lines show the monthly climatological mean.

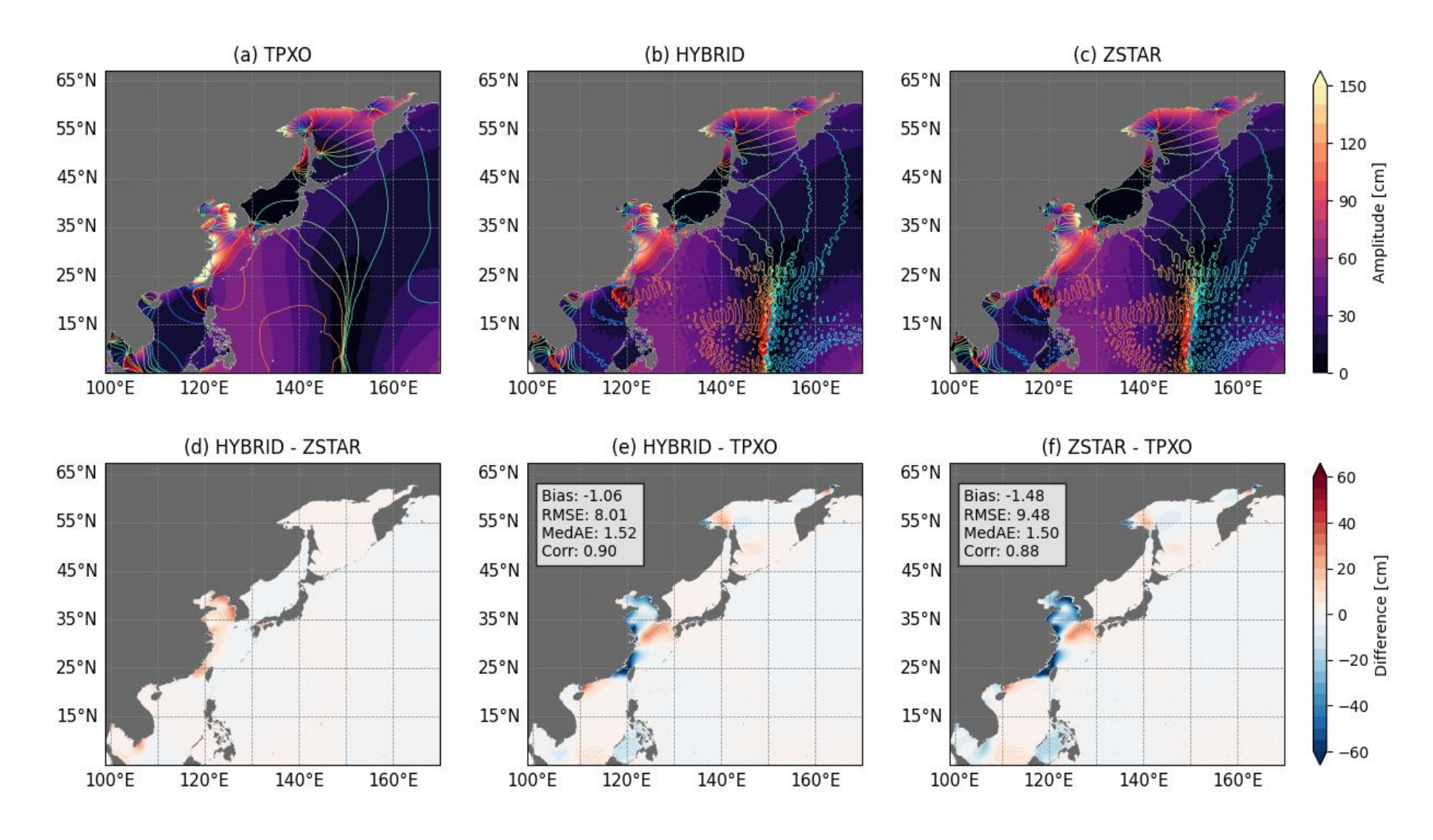


Figure 19. Semidiurnal M2 tidal amplitude and phase from TPXO data, HYBRID, and ZSTAR simulations. Shaded contours represent tidal amplitude, while overlaid coloured contours show tidal phase for M2 (a–c). Panels below display tidal amplitude differences: (a) HYBRID vs. ZSTAR, (b) HYBRID vs. TPXO, and (c) ZSTAR vs. TPXO. Metrics include Bias, RMSE, MedAE, and Corr.

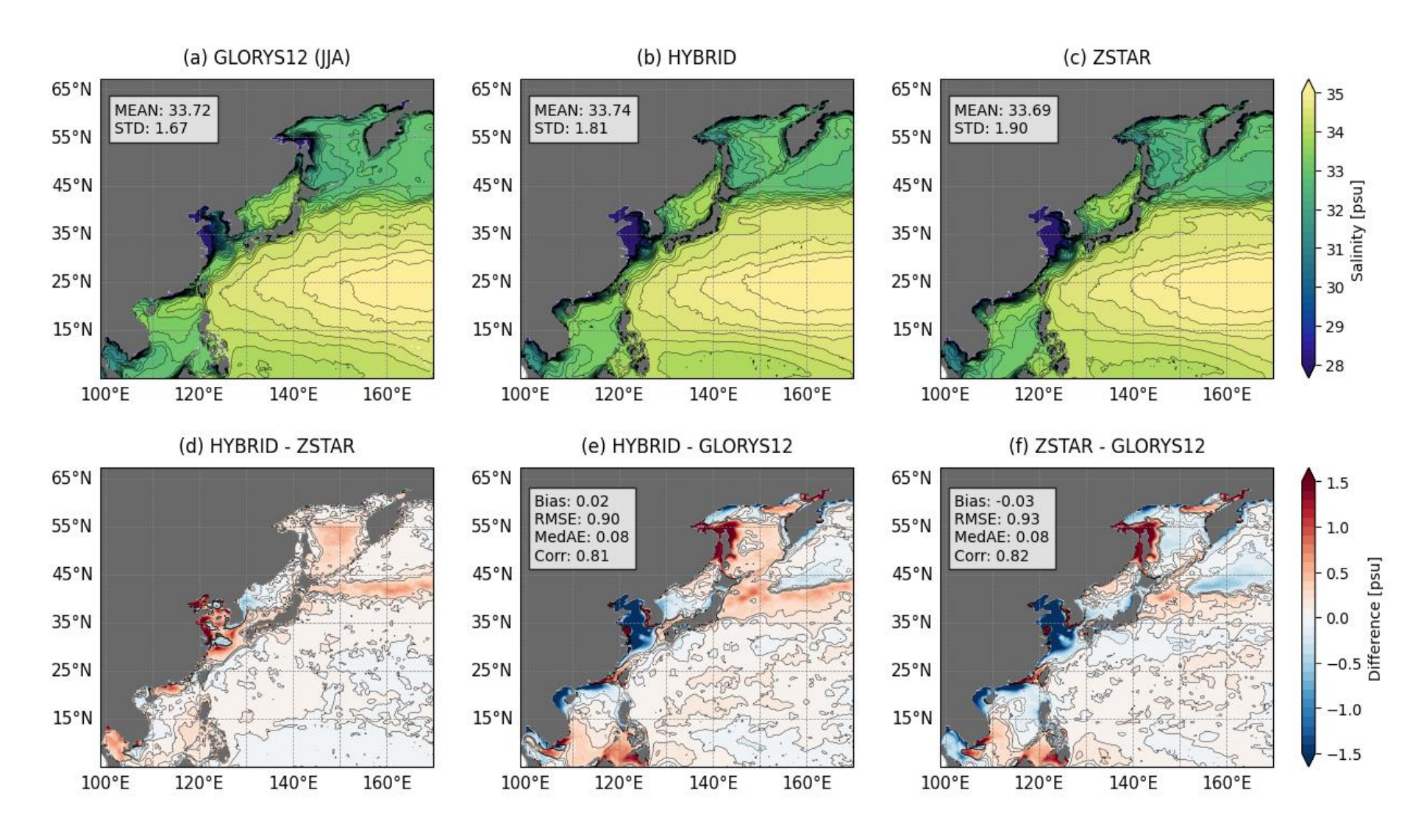


Figure S1. Boreal summer (JJA) mean sea surface salinity (SSS) distributions from GLORYS12 reanalysis and HYBRID and ZSTAR simulations. (a–c) Spatial SSS distributions with corresponding means and standard deviations (STD). (d) Differences between HYBRID and ZSTAR. (e, f) Biases relative to GLORYS12, including mean bias, RMSE, MedAE, and Corr. Contour lines in (d–f) indicate SSS biases ranging from -0.1 to 0.1 psu at 0.1 psu intervals.

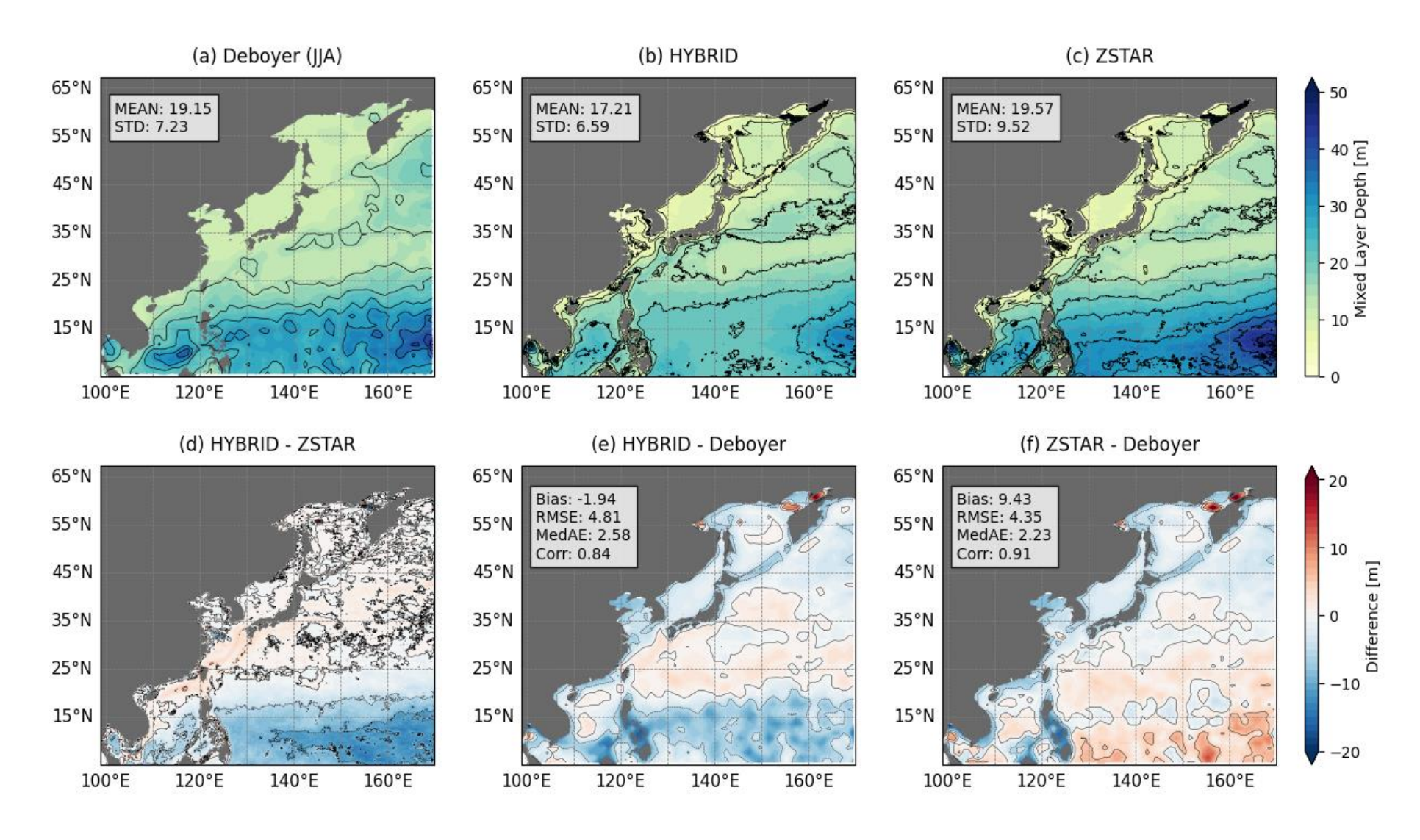


Figure S2. Boreal summer (JJA) mean mixed layer depth (MLD) distributions from de Boyer Montégut and HYBRID and ZSTAR simulations. (a–c) Spatial MLD distributions with corresponding means and standard deviations (STD). (d) Differences between HYBRID and ZSTAR. (e, f) Biases relative to de Boyer Montégut, including mean bias, RMSE, MedAE, and Corr. Contour lines in (d–f) indicate MLD biases ranging from -0.1 to 0.1 m at 0.1 m intervals.

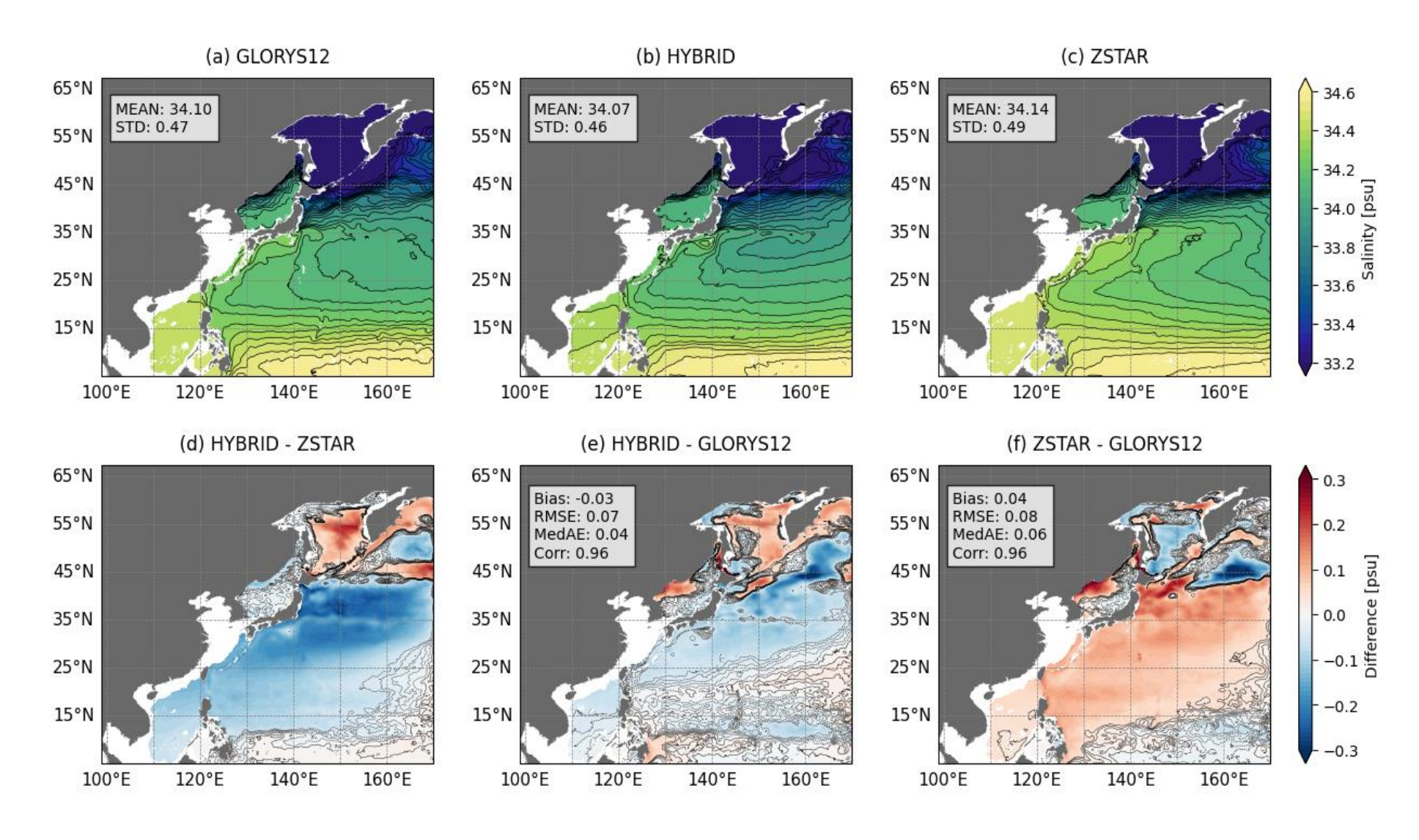


Figure S3. Salinity distributions at depths corresponding to σ_2 = 35.8 from (a) GLORYS12, (b) HYBRID, and (c) ZSTAR simulations, along with their respective means and standard deviations (STD). (d) Differences between HYBRID and ZSTAR. (e, f) Biases relative to GLORYS12, including mean bias, RMSE, MedAE, and Corr. Contour lines in (d–f) indicate salinity biases ranging from -0.1 to 0.1 psu at 0.1 psu intervals.

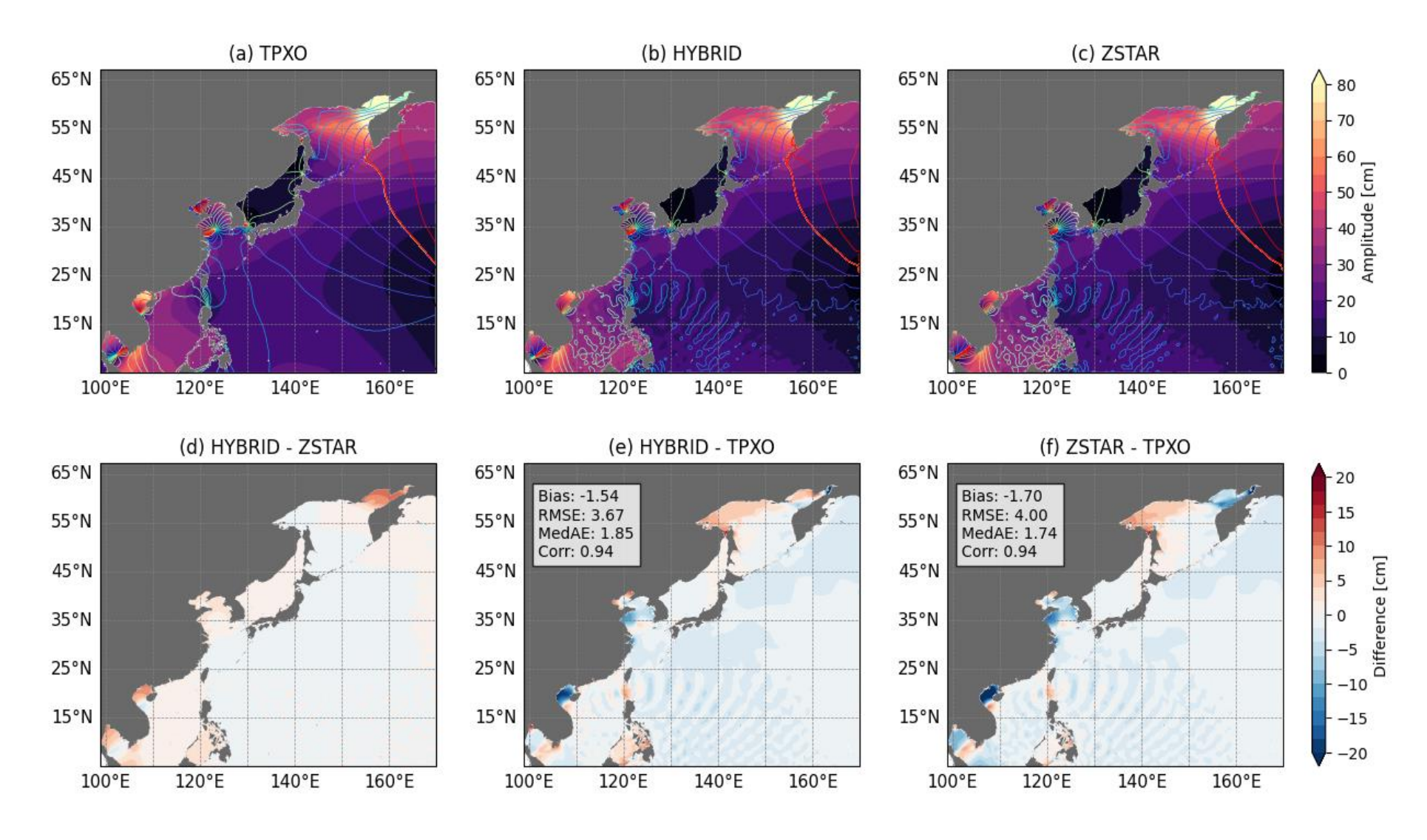


Figure S4. Diurnal K1 tidal amplitude and phase from TPXO data, HYBRID, and ZSTAR simulations. Shaded contours represent tidal amplitude, while overlaid coloured contours show tidal phase for K1 (a–c). Panels below display tidal amplitude differences: (a) HYBRID vs. ZSTAR, (b) HYBRID vs. TPXO, and (c) ZSTAR vs. TPXO. Metrics include mean bias, RMSE, MedAE, and Corr.

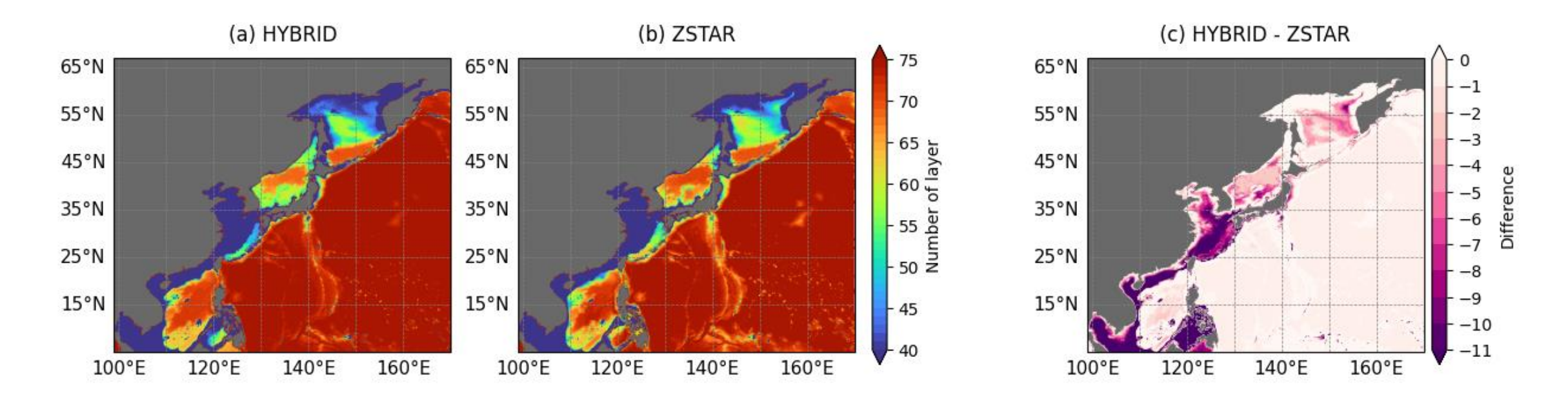


Figure S5. Spatial distribution of active layers in HYBRID and ZSTAR on December 22, 2012. (a, b) Number of active layers in HYBRID and ZSTAR, respectively, where an active layer is defined as having a thickness greater than 0.001 m. (c) Difference (HYBRID - ZSTAR).

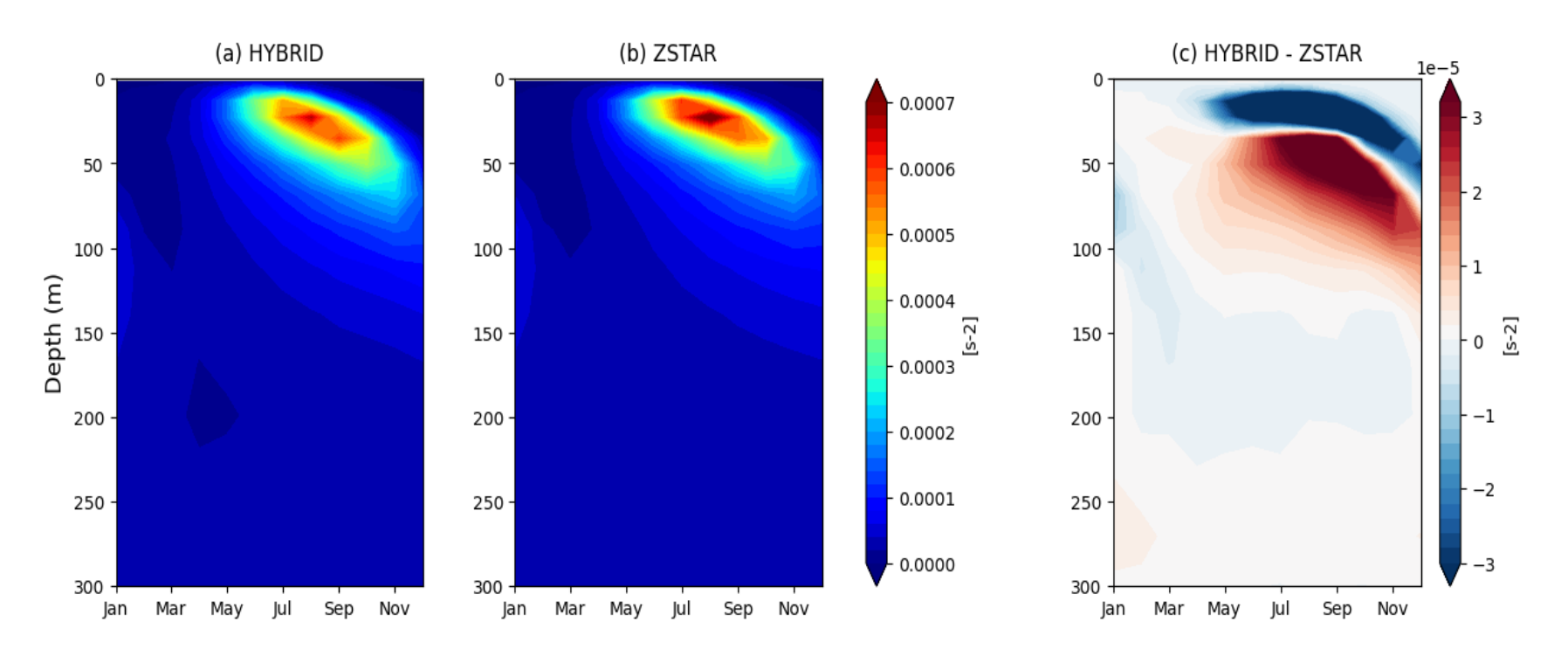


Figure S6. Seasonal evolution of buoyancy frequency squared (N², s⁻²) averaged over 25°-35°N and 140°-160°E for (a) HYBRID, (b) ZSTAR, and (c) their difference (HYBRID - ZSTAR).

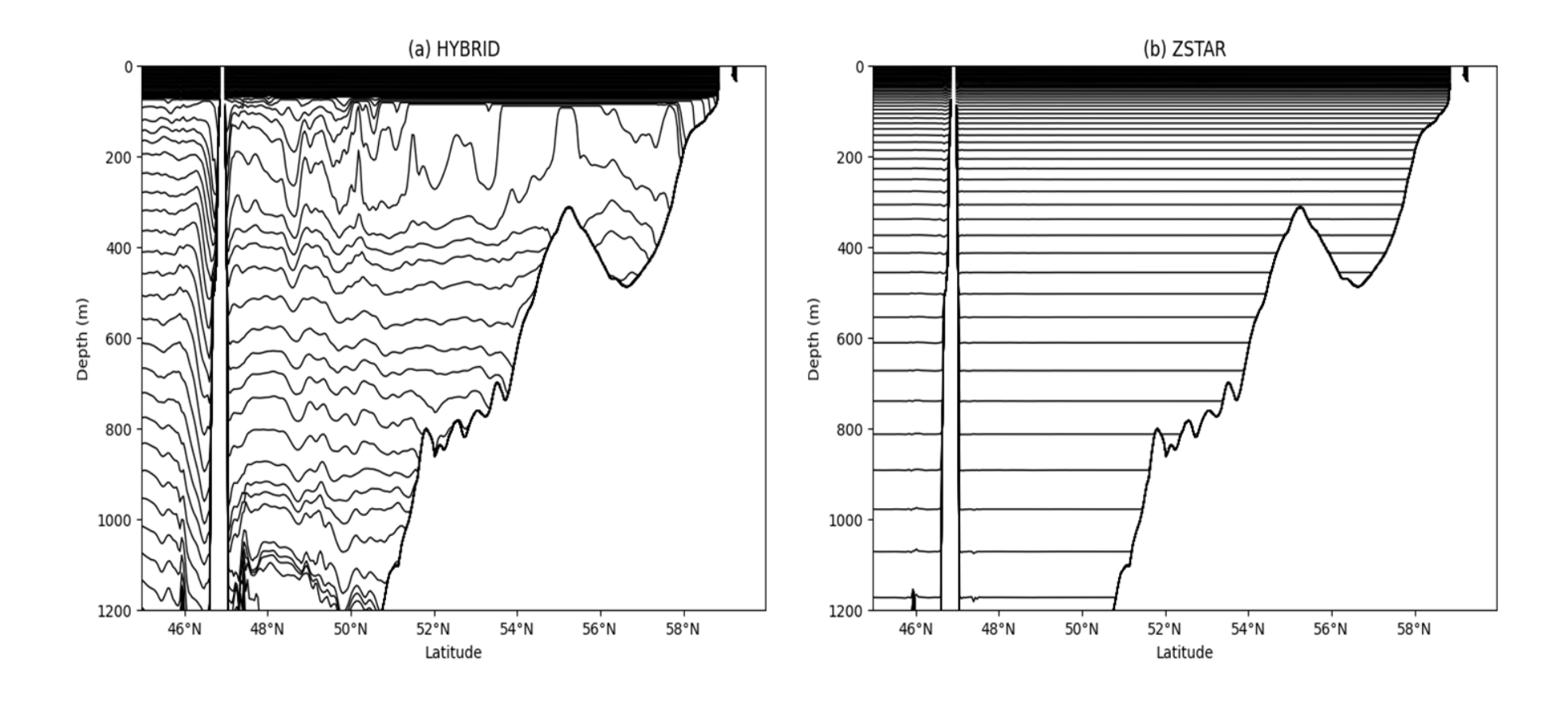


Figure S7. Model interfaces along 152°E in the Sea of Okhotsk for (a) HYBRID and (b) ZSTAR.

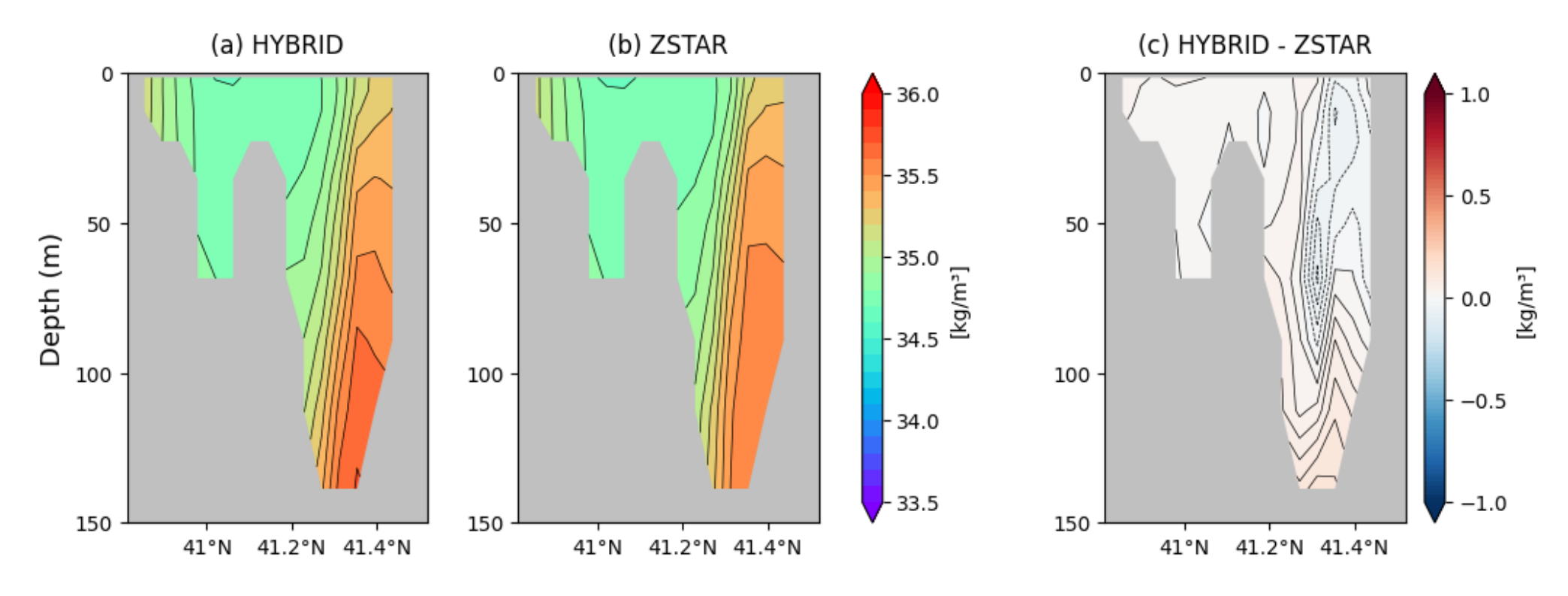


Figure S8. Meridional section of potential density (σ₂, referenced to 2000 m) across the Tsugaru Strait, averaged over 2012. (a) ZSTAR, (b) HYBRID, and (c) HYBRID–ZSTAR difference.

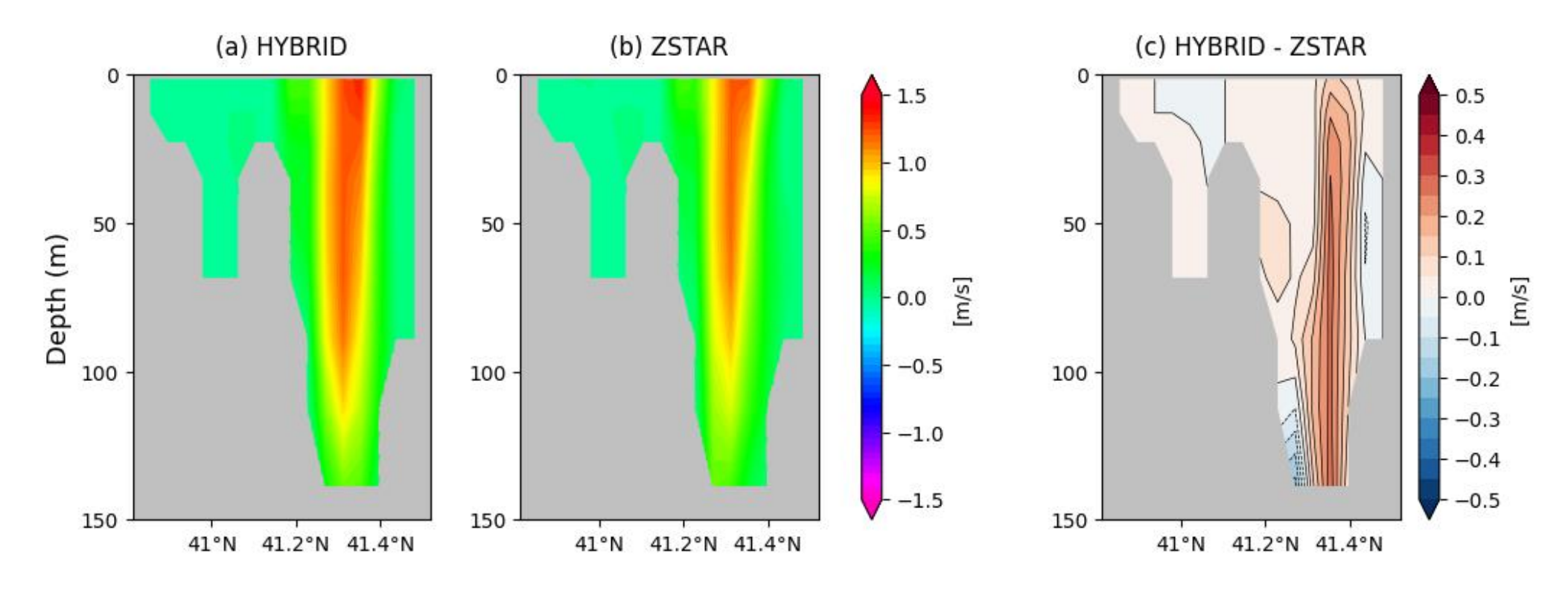


Figure S9. Meridional section of along-strait velocity (U) across the Tsugaru Strait, averaged over 2012. (a) ZSTAR, (b) HYBRID, and (c) HYBRID–ZSTAR difference.